

## PUBLISHED VERSION

David J Ottaway, Lachlan Harris, and Peter J. Veitch  
**Short-pulse actively Q-switched Er:YAG lasers**  
Optics Express, 2016; 24(14):15341-15350

© 2016 Optical Society of America. Open Access - CC BY license.

Published version <http://dx.doi.org/10.1364/OE.24.015341>

### PERMISSIONS

**Rights url:** [https://www.osapublishing.org/submit/review/copyright\\_permissions.cfm#](https://www.osapublishing.org/submit/review/copyright_permissions.cfm#)

#### Creative Commons Licensing

OSA is aware that some authors, as a condition of their funding, must publish their work under a Creative Commons license. We therefore offer a CC BY license for authors who indicate that their work is funded by agencies that we have confirmed have this requirement. Authors must enter their funder(s) during the manuscript submission process. At that point, if appropriate, the CC BY license option will be available to select for an additional fee.

Any subsequent reuse or distribution of content licensed under CC BY must maintain attribution to the author(s) and the published article's title, journal citation, and DOI.

<http://creativecommons.org/licenses/by/4.0/>



This is a human-readable summary of (and not a substitute for) the [license](#).

[Disclaimer](#)



#### You are free to:

**Share** — copy and redistribute the material in any medium or format

**Adapt** — remix, transform, and build upon the material  
for any purpose, even commercially.

The licensor cannot revoke these freedoms as long as you follow the license terms.

#### Under the following terms:



**Attribution** — You must give **appropriate credit**, provide a link to the license, and **indicate if changes were made**. You may do so in any reasonable manner, but not in any way that suggests the licensor endorses you or your use.

**No additional restrictions** — You may not apply legal terms or **technological measures** that legally restrict others from doing anything the license permits.

15 September 2016

<http://hdl.handle.net/2440/101205>

# Short-pulse actively Q-switched Er:YAG lasers

DAVID J OTTAWAY,\* LACHLAN HARRIS, AND PETER J. VEITCH

*Department of Physics and Institute of Photonics and Advanced Sensing,  
The University of Adelaide, Adelaide, South Australia, Australia*  
\*[david.ottaway@adelaide.edu.au](mailto:david.ottaway@adelaide.edu.au)

**Abstract:** We report the shortest duration pulses obtained to date from an actively Q-switched Er:YAG laser pumped by a low spectral and spatial brightness laser diode. The 14.5 ns, 6 mJ pulses were obtained using a 1470 nm laser diode end-pumped co-planar folded zigzag slab architecture. We also present an analytical model that accurately predicts the pulse energy-duration product achievable from virtually all Q-switched Er:YAG lasers and high repetition rate quasi-three-level Q-switched lasers in general.

© 2016 Optical Society of America

**OCIS codes:** (140.3500) Lasers, erbium; (140.3540) Lasers, Q-switched; (140.3070) Infrared and far-infrared lasers; (140.3580) Lasers, solid-state.

## References and links

1. S. D. Setzler, M. P. Francis, Y. E. Young, J. R. Konves, and E. P. Chicklis, "Resonantly pumped eyesafe erbium lasers," *IEEE J. Sel. Top. Quantum Electron.* **11**, 645–657 (2005).
2. W. Koechner, *Solid-State Laser Engineering* (Springer, 2013).
3. W. G. Wagner and B. A. Lengyel, "Evolution of the giant pulse in a laser," *J. Appl. Phys.* **34**, 2040–2046 (1963).
4. J. J. Degnan, "Theory of the optimally coupled Q-switched laser," *IEEE J. Quantum Electron.* **25**, 214–220 (1989).
5. J. J. Degnan, "Optimization of passively Q-switched lasers," *IEEE J. Quantum Electron.* **31**, 1890–1901 (1995).
6. P. Li, Q. Wang, and D. Gao, "Maximum peak power generation from Q-switched lasers," *Opt. Laser Technol.* **31**, 247–250 (1999).
7. V.E. Kisel, A.S. Yasukevich, N.V. Kondratyuk and N.V.Kuleshov, "Diode-pumped passively Q-switched high-repetition-rate Yb microchip laser" *Quantum Electron.* **39**, 1018 (2009).
8. R. J. Beach, "Optimization of quasi-three-level end-pumped Q-switched lasers," *IEEE J. Quantum Electron.* **31**, 1606–1613 (1995).
9. R. C. Stoneman, R. Hartman, E. A. Schneider, A. I. Malm, S. R. Vitorino, C. G. Garvin, J. V. Pelk, S. M. Hannon, and S. W. Henderson, "Eyesafe 1.6  $\mu\text{m}$  Er: YAG transmitters for coherent laser radar," in *Proceedings of 14th Coherent Laser Radar Conference (CLRC XIV)* (2007).
10. R. D. Stultz, V. Leyva, and K. Spariosu, "Short pulse, high-repetition rate, passively Q-switched Er: yttrium-aluminum-garnet laser at 1.6 microns," *Appl. Phys. Lett.* **87**, 1118 (2005).
11. J. Kim, J. Sahu, and W. Clarkson, "High-energy Q-switched operation of a fiber-laser-pumped Er: YAG laser," *Appl. Phys. B* **105**, 263–267 (2011).
12. S. D. Setzler, Y. E. Young, K. J. Snell, P. A. Budni, T. M. Pollak, and E. P. Chicklis, "High-peak-power erbium lasers resonantly pumped by fiber lasers," *Proc. SPIE* **5332**, 85–96 (2004).
13. M. Wang, J. Meng, X. Hou, and W. Chen, "In-band pumped polarized, narrow-linewidth Er: YAG laser at 1645 nm," *Appl. Opt.* **53**, 7153–7156 (2014).
14. N. Chang, N. Simakov, D. Hosken, J. Munch, D. Ottaway, and P. Veitch, "Resonantly diode-pumped continuous-wave and Q-switched Er: YAG laser at 1645 nm," *Opt. Express* **18**, 13673–13678 (2010).
15. I. Kudryashov and A. Katsnelson, "1645-nm Q-switched Er: YAG laser with in-band diode pumping," in *SPIE Defense, Security, and Sensing*, (SPIE, 2010), pp. 76860B–76860B.
16. J. Richards and A. McInnes, "Versatile, efficient, diode-pumped miniature slab laser," *Opt. Lett.* **20**, 371–373 (1995).
17. J. Eggleston, L. Frantz, and H. Injeyan, "Deviation of the Frantz-Nodvik equation for zig-zag optical path, slab geometry laser amplifiers," *IEEE J. Quantum Electron.* **25**, 1855–1862 (1989).
18. R. B. Kay and D. Poullos, "Q-switched rate equations for diode side-pumped slab and zigzag slab lasers including gaussian beam shapes," *IEEE J. Quantum Electron.* **41**, 1278–1284 (2005).
19. R. B. Kay, D. Poullos, D. B. Coyle, P. R. Stysley, and G. B. Clarke, "Derivation of the Frantz-Nodvik equation for diode-side-pumped zigzag slab laser amplifiers with gaussian laser mode and pump beam shapes," *IEEE J. Quantum Electron.* **47**, 745–749 (2011).

## 1. Introduction

Compact and efficient lasers that produce short duration, high energy pulses are required for a variety of field-based laser radar applications, including "range-finders" for which the pulse duration determines the range resolution and the peak power determines the maximum range. Direct generation of such pulses at 1617 nm or 1645 nm using Q-switched Er:YAG lasers would allow replacement of such sources that currently use non-linear materials to frequency down-convert short-duration pulses at 1  $\mu\text{m}$  to the eye-safe band (1.5-1.8  $\mu\text{m}$ ). However, short durations are difficult to achieve using Er:YAG because it has inherently low gain as the ions in the upper lasing state are spread between seven relatively closely spaced Stark-shifted levels [1].

There have been many theoretical studies of Q-switched lasers [2-11] but generally they have focused on optimizing the efficiency rather than minimizing the pulse duration. Equations describing the operation of Q-switched lasers were first outlined by Wagner and Lengyel [3]. However, these equations are transcendental and required complicated numerical solutions. Degnan [4, 5] generalized the equations to quasi-three-level lasers by including an inversion reduction factor and used Lagrange multipliers to obtain simpler expressions for the pulse properties for the case where the laser has the optimum output coupling. Li et al. [6] recast Degnan's approach to consider the effect of optimizing the reflectivity of the output coupler to maximize the peak output power and showed that it could be increased. Kisel et al. [7] linearized the equations developed for passive Q-switching to develop analytical solutions for pulse repetition frequency of such a laser in the high pulse repetition frequency limit. Beach [8] adopted a different approach and developed equations that did not insist on optimum output coupling and could be evaluated easily using numerical techniques so that design sensitivity studies could be performed. In this paper we study the case of Er:YAG lasers that are actively Q-switched and derive a simple relationship between pulse energy and duration that is applicable to any actively Q-switched Er:YAG lasers and any actively Q-switched quasi-three-level laser operating in the high repetition frequency limit. We used this insight to develop a new laser that produced the shortest duration pulses from an actively Q-switched laser.

The shortest duration pulsed Er:YAG laser reported so far yielded 1.1 ns, 1.6 mJ pulses, produced using an injection-seeded and cavity dumped master-oscillator-power-amplifier system, an architecture that was chosen to prevent optical damage [9]. The gain media were pumped by Er-Yb doped fiber lasers (EDFL) tuned to the 1532 nm absorption line of Er:YAG by an external cavity. Passively Q-switching an EDFL-pumped Er:YAG laser using a ZnSe saturable absorber yielded 6.8 ns, 0.24 mJ pulses [10]. This short pulse duration was achieved because the passive Q-switch was very small, enabling the use of an extremely compact resonator. However, the damage threshold of ZnSe is low, which limits the power scaling of this approach.

The shortest pulses produced by an actively Q-switched oscillator have used EDFL-pumping, yielding pulse durations and energies of 20 ns and 30.5 mJ [11] and 21 ns and 3.4 mJ [12]. It would thus appear that passively Q-switched Er:YAG lasers can generate ca. 7 ns pulses but perhaps only with low energies, and the shortest pulse duration for an actively Q-switched Er:YAG laser is ca. 20 ns.

Compact and efficient Q-switched Er:YAG lasers should be achievable using direct laser-diode pumping but short duration and high energy pulses from such systems have yet to be demonstrated. An acousto-optically-Q-switched Er:YAG laser pumped using a fiber-coupled bandwidth-narrowed 1532 nm laser diode produced 95 ns, 12 mJ pulses [13]. Diode pumping using a close-coupled broadband 1470 nm diode has also been used to demonstrate 100 ns, 2.3 mJ pulses at 250 Hz Pulse Repetition Frequency (PRF) with a total optical-to-optical efficiency of 2.5% [14]. Diode pumping using a spectrally narrowed 1470 nm laser diode has been demonstrated to produce 27 ns, 10.5 mJ pulses at 20 Hz PRF [15].

We report the results of an investigation of Q-switched Er:YAG lasers with an emphasis on minimizing the pulse duration, rather than optimizing the efficiency. Our approach provides a

new simple expression for the pulses produced by short-duration Q-switched lasers with quasi-three-level gain media. Importantly, we validate these expressions and demonstrate the shortest duration pulses yet achieved from an actively Q-switched Er:YAG laser at 1.6  $\mu\text{m}$ .

A laser gain medium architecture with high gain was crucial to obtaining these results as it allowed the use of low reflectance output couplers which reduces the ratio of intra-cavity power to output power and hence allowed us to avoid optical damage. Thus, we used a folded zigzag slab architecture [16], which allows end-pumping and thus low doping. Zigzag slabs offer additional advantages, including reduced thermal lensing, increased gain and easier mounting [2]. However, they also add some theoretical complexity because of the overlapping laser fields. Eggleston et al. [17] addressed this issue by using a so-called “average flux approximation”. Kay et al. used this technique for non-uniformly-pumped zigzag slabs, developing both a numerical approach [18] and an analytical expression [19] for calculating the output energy assuming a Gaussian-intensity profile pulse. We assume uniform pumping, as the pump absorption bleaches due to the low doping and thus the population inversion is more uniformly distributed along the gain medium. We also introduce an “overlap factor” that can be adjusted to suit the gain medium architecture.

The Er:YAG laser we describe here is a compact electro-optically-Q-switched laser that is pumped using a broadband single-bar 1470 nm diode and produces 14.5 ns, 6 mJ pulses.

The outline of the paper is as follows: in Section 2 we present a new model that gives a simple analytical relationship between pulse energy and duration. In Section 3 we describe the laser system that was used to validate this new model and demonstrate short pulses from an actively Q-switched laser. We compare the properties of observed pulses with predictions of the model in Section 4.

## 2. Theory

The Q-switched laser model we present in this section is an extension of the work by Degnan [4]. It assumes that the gain medium has only two energy manifolds whose combined population is constant, ie  $N_{eff} \equiv N_1 + N_2$  where  $N_1$  and  $N_2$  are the population densities of lower and upper lasing manifolds respectively. This is a valid assumption for resonant pumping if the effect of energy transfer processes and excited state absorption are negligible due to low dopant concentrations, in which case  $N_{eff}$  is the total dopant concentration. The aforementioned assumption can still hold if energy transfer processes are significant during the pumping time but insignificant during evolution of the Q-switch pulse which is much shorter. In this case  $N_{eff}$  will be less than the total dopant concentration.

The time dependent behavior of the photon number density of the spatially averaged laser mode traveling in one direction within the resonator (Eq. 1 of [4]) is given by

$$\frac{d\phi}{dt} = \left( \frac{\sigma L(f_2 N_2 - f_1 N_1)}{t_r} - \frac{1}{t_c} \right) \phi \quad (1)$$

where  $\sigma$  is the cross section of the lasing transition,  $L$  is the round-trip path length within the gain medium,  $t_r$  is the resonator round-trip time,  $f_2$  and  $f_1$  are the Boltzmann factors for the upper and lower lasing states, and the cavity lifetime  $t_c$  is given by

$$t_c = - \frac{t_r}{\delta + \ln(R)} \quad (2)$$

where  $R$  is the reflectivity of the output coupler,  $\delta = \ln(1 - L_i)$  and  $L_i$  is the fractional round trip loss within the resonator

The evolution of the population densities during a Q-switched pulse is

$$\frac{dN_2}{dt} = - \frac{dN_1}{dt} = - \sigma B c \phi (f_2 N_2 - f_1 N_1) \quad (3)$$

where  $c$  is the speed of light in a vacuum and we have introduced a new factor  $B$  that accounts for the laser mode overlapping with itself in the gain medium and therefore the effective intensity that interacts with the population inversion. We expect  $B = 1$  for a non-zigzag ring resonator,  $B = 2$  for a non-zigzag linear resonator and  $B = 4$  for a zigzag linear resonator.

Combining Eq. (1) and Eq. (3) gives

$$\frac{d\phi}{dN_2} = -\frac{L}{Bct_r} + \frac{1}{\sigma Bc(f_2N_2 - f_1N_1)t_c} \quad (4)$$

Integrating Eq. (4), defining  $N_2 = N_i$  at the start of the pulse and assuming  $\phi(N_2 = N_i) = 0$ , gives

$$\phi(N_2) = \frac{(N_i - N_2)L}{Bct_r} - \frac{1}{t_c\sigma Bc(f_1 + f_2)} \ln\left(\frac{f_2N_i + f_1N_i - f_1N_{eff}}{f_2N_2 + f_1N_2 - f_1N_{eff}}\right) \quad (5)$$

At the end of the pulse  $\phi = 0$  and  $N_2 = N_f$ . Thus

$$0 = (N_i - N_f) - \frac{t_r}{\sigma Lt_c(f_1 + f_2)} \ln\left(\frac{f_2N_i + f_1N_i - f_1N_{eff}}{f_2N_f + f_1N_f - f_1N_{eff}}\right) \quad (6)$$

At the peak of the pulse the round-trip gain is 1 and hence  $\frac{d\phi}{dt} = 0$  and  $N_2 = N_t$ , the threshold population density. Thus Eq. (1) gives

$$N_t = \frac{f_1}{f_1 + f_2} N_{eff} + \frac{\delta - \ln(R)}{\sigma L(f_1 + f_2)} = N_{trans} + \frac{\delta - \ln(R)}{\sigma L(f_1 + f_2)} \quad (7)$$

where  $N_{trans}$  is the upper state population density at which the gain medium becomes transparent to the laser radiation.

Equation (6) is transcendental and must be solved numerically to determine  $N_f$  for a given  $N_i$ . However, if the initial population density of the upper manifold ( $N_i$ ) is moderately larger than the threshold population density ( $N_t$ ) then, as shown in Appendix A,

$$N_t - N_f = N_i - N_t \quad (8)$$

which can be written  $\Delta N_f = \Delta N_i$  where  $\Delta N_i = N_i - N_t$  and  $\Delta N_f = N_t - N_f$ .

A typical numerical solution of Eq. (6) and Eq. (7), for the parameters shown in Table 1, is plotted in Fig. 1 (left). This figure shows, as expected, that if  $\Delta N_i$  is small then Eq. (8) holds. The range of  $N_i$  for which this approximation is valid will increase as the reflectivity of the output coupler decreases, as  $N_t - N_{trans}$  increases.

If  $N_i \gg N_t$  then the final population density ( $N_f$ ) asymptotes towards  $N_{trans}$ , the smallest value of  $N_f$  for which Eq. (6) is real valued (ie  $f_2N_f + f_1N_f - f_1N_{eff} > 0$ ).

Table 1. Parameters used in the numerical simulation

Parameter	Value	Parameter	Value
$\sigma_{1645}$	$2.7 \times 10^{-20} \text{ cm}^2$	$R$	0.4
$t_r$	1.33 ns	$L_i$	0.1
$A$	$2.6 \times 10^{-3} \text{ cm}^2$	$B$	4
$f_1$	0.02	$f_2$	0.21
$L$	10.7 cm		

We now determine the output power, pulse energy and duration by considering the evolution of the pulse. The output power is related to the photon density (Eq. A.12 of [4]) by

$$P(N_2) = -h\gamma A c \ln(R) \phi(N_2) \quad (9)$$

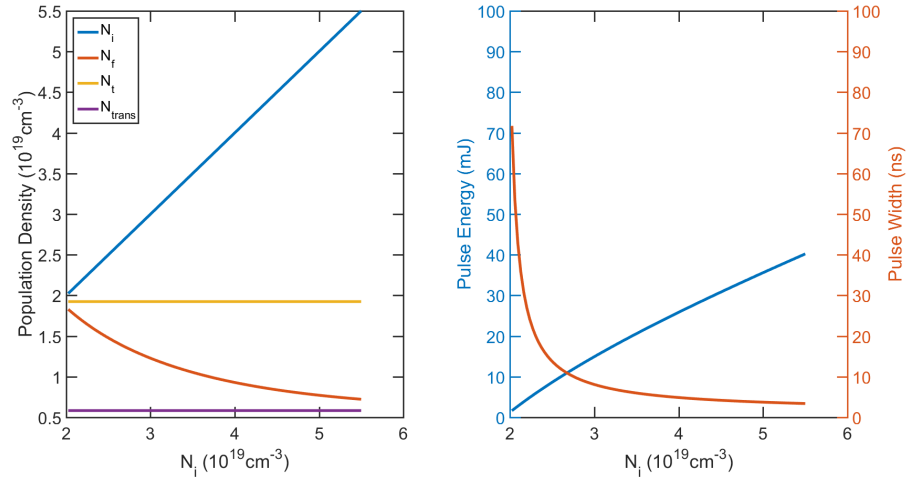


Fig. 1. Left: A plot of the upper manifold population densities at the start ( $N_i$ ) and end ( $N_f$ ) of the pulse for a given initial population density ( $N_i$ ). Right: A plot of the dependence of the pulse energy and width on the initial population density.

where  $\phi(N_2)$  is given by Eq. (5),  $h$  is Planck's constant and  $\gamma$  is the frequency of the laser light. The energy of the output pulse is obtained by integrating Eq. (9), giving

$$E = \int_{N_i}^{N_f} P(N_2) dN_2 = -\frac{h\gamma A \ln(R)}{\sigma B(f_1 + f_2)} \ln\left(\frac{f_2 N_i + f_1 N_i - f_1 N_{eff}}{f_2 N_f + f_1 N_f - f_1 N_{eff}}\right) \quad (10)$$

This equation can be simplified by combining it with Eq. (6) giving

$$E = \frac{-h\gamma A L \ln(R)}{B} \frac{N_i - N_f}{\delta - \ln(R)} \quad (11)$$

The peak power occurs when  $N_2 = N_i$  and hence is given by

$$P_p = \frac{-h\gamma A \ln(R)}{B} \times \left( \frac{(N_i - N_i)L}{t_r} - \frac{1}{\sigma t_c (f_1 + f_2)} \ln\left(\frac{f_2 N_i + f_1 N_i - f_1 N_{eff}}{f_2 N_i + f_1 N_i - f_1 N_{eff}}\right) \right) \quad (12)$$

This equation can be simplified by using a series expansion in the small  $\Delta N_i$  regime, giving

$$P_p = \frac{-\ln(R)}{\delta - \ln(R)} \frac{h\gamma A \sigma L^2 (f_2 + f_1) (N_i - N_i)^2}{2B t_r} \quad (13)$$

A characteristic pulse width ( $\Delta t$ ) can be calculated, following [4], by dividing the pulse energy by the peak power. The dependence of the pulse energy and width on the initial population density in the upper manifold is plotted in Fig. 1 (Right).

In the small  $\Delta N_i$  limit

$$E \times \Delta t = \frac{E^2}{P_{peak}} = \frac{-8h\gamma A \ln(R) t_c}{B(f_1 + f_2)\sigma} = \frac{8h\gamma A t_r}{B(f_1 + f_2)\sigma} \frac{-\ln(R)}{\delta - \ln(R)} \quad (14)$$

and thus  $\Delta t^{-1} \propto E$  and  $E \times \Delta t / A \propto t_r$

The inverse pulse width and the pulse energy are plotted in Fig. 2 for the complete numerical solution and the small  $\Delta N_i$  solution, using the parameters listed in Table 1. Fig. 2 shows that the small  $\Delta N_i$  approximation is accurate to within 10% to an output energy of 30 mJ. An output energy that is significantly higher than the damage threshold for this laser.

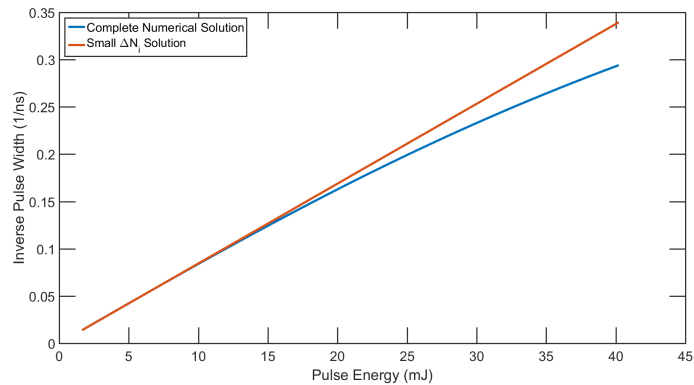


Fig. 2. Comparison of the pulse duration versus pulse energy for the complete numerical solution and the small  $\Delta N_i$  solution described in Eq. (14)

### 3. Laser description

A schematic of the laser is shown in Fig. 3. The 0.5 at.% Er:YAG gain medium uses a coplanar-folded-zigzag-slab (CPFS) architecture [16], which has Brewster-angled entrance and exit faces. This geometry maximizes the gain-length product for a given absorbed pump density because the laser mode passes the same volume four times. It also allows close-coupled end pumping that conveniently separates the lasing mode and the pump light without the need for dichroic optical coatings on the slab. Two slab lengths were used: 21 mm and 35 mm. Both slabs were 2.0 mm wide (in zigzag plane), 4.0 mm high and were mounted in a laser head consisting of two water-cooled copper blocks. Indium was placed between the slab and copper blocks to provide stress relief and facilitate cooling.

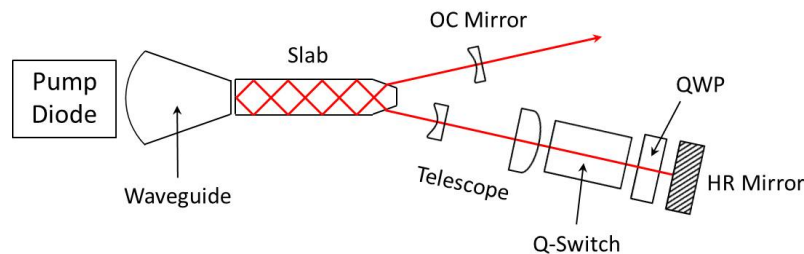


Fig. 3. Schematic of the Q-switched laser incorporating the CPFS slab.

The roundtrip loss of these slabs were measured using a 1319 nm wavelength CW laser. This wavelength was used to separate the scattering loss from the ground state re-absorption that occurs when a wavelength of 1.6  $\mu\text{m}$  is used. It was found that the round-trip loss at this wavelength was 10% for the shorter 21 mm slab and 14% for the longer 35 mm slab. This relatively high loss was attributed to the high number of internal bounces (21 for short slab and 35 for long slab) required for this geometry.

The gain medium was pumped by a single-array fast-axis-collimated diode, the output of which was guided into the slab using a tapered lens duct, producing a 0.6 mm high pumped region. The laser resonator used a flat HR mirror and 20 cm radius-of-curvature output coupler (OC). A telescope is used to expand the intra-cavity mode and decrease the fluence at the RTP Q-switch and quarter-wave plate (QWP).

The laser was initially tested in long-pulse mode using 10 ms pump pulses at 12 Hz repetition rate with peak pump powers of up to 60 W, corresponding to a 600 mJ pump pulse. A comparison of the output pulse energy for both slabs against a range of output coupler reflectivities is shown in Fig. 4 and 5.

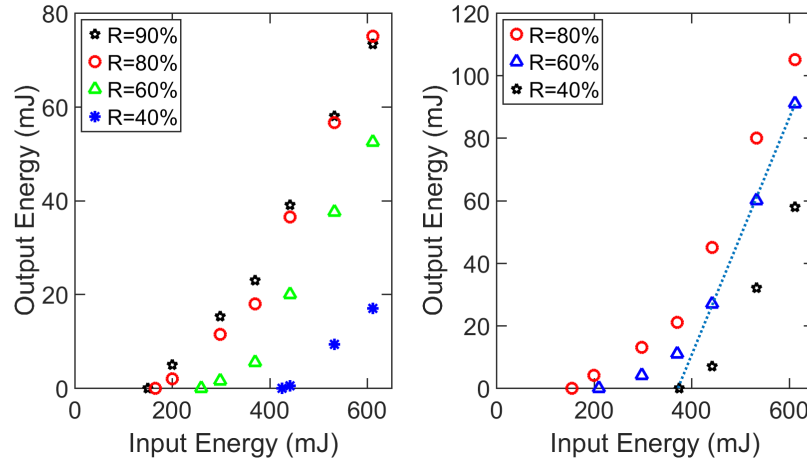


Fig. 4. Plot of the output energy versus incident energy for the laser in long-pulse mode for the short 21 mm slab (Left) and the long slab 35 mm slab (Right). The slope of the solid line corresponds to a slope efficiency of 40%.

The threshold pump energy is relatively large for both slabs due to the quasi-three-level nature of Er:YAG. A significant fraction of this energy is needed to make the Er:YAG transparent, the remainder is used to overcome output coupling and scatter losses. Both systems have similar threshold energies because the short slab does not absorb all of the pump light.

The additional gain and stored energy in the longer slab allowed the use of a less reflective output coupler, resulting in increased efficiency, as shown in Fig. 5. The highest slope efficiency was achieved using a  $R = 60\%$  output coupler as shown by the solid line in Fig. 4 (Right); the 40% slope efficiency compared to the energy emitted by the pump source is only slight less than that reported by Setzler [12] and yet was achieved using a cheap low spectral and spatial brightness laser diode pump source rather than an EDFL pump source.

It is thus apparent that the CPFS architecture enables a high-round-trip gain and higher output coupling with minimal loss of slope efficiency. Unfortunately, the extra-gain of the long CPFS slab will not significantly reduce the duration of the Q-switched pulses compared to rod architectures [12] as the resonator round-trip time is also increased.

Thus, we chose to use a  $R = 40\%$  output coupler in the Q-switched laser to further reduce the intra-cavity peak power and enable increased pulse energy. The shortest duration pulses were achieved using the short slab, with duration of  $14.5 \pm 0.2$  ns and average pulse energy of 6 mJ at 12 Hz pulse repetition frequency. A plot of this pulse is shown in Fig. 6. A plot of the pulse duration and output energy versus input energy for this slab is included as Fig. 7

Er:YAG lasers can operate at either 1617 nm or 1645 nm, as determined by the upper manifold population density at the start of the pulse. The 1617 nm transition has a higher cross section but higher re-absorption losses, which reduce as ions are removed from the ground state. Thus, lasing occurs at 1617 nm when the average upper manifold population density exceeds

$$N = \frac{N_{eff}(\sigma_{1617}f_{1@1617} - \sigma_{1645}f_{1@1645})}{\sigma_{1645}(f_{2@1645} + f_{1@1645}) - \sigma_{1617}(f_{2@1617} + f_{1@1617})} \quad (15)$$



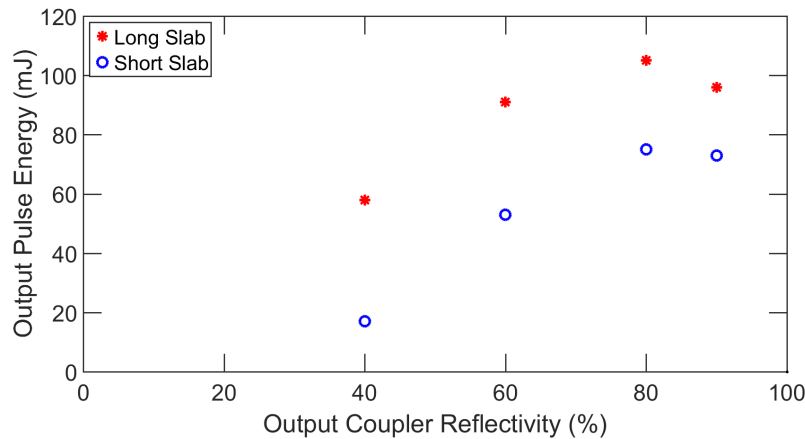


Fig. 5. Output pulse energy in long pulse-mode for both slabs versus output coupler reflectivity for an input pump pulse energy of 600 mJ.

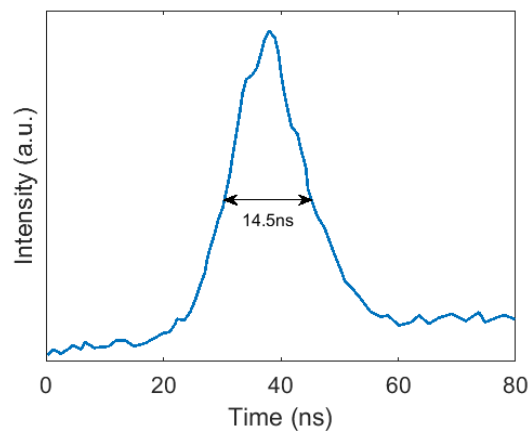


Fig. 6. Plot of the shape of the shortest duration pulse. The pulse shape was measured using an InGaAs photodiode with a 200 ps rise time and a 200 MHz bandwidth oscilloscope.

The required gain at threshold is dominated by the output coupling fraction when its value is high. In this case the shorter slab requires a greater population inversion to achieve the same gain since its length is reduced. Hence it will lase at 1617 nm whilst the longer slab will tend to lase at 1645 nm.

#### 4. Comparison of measured and predicted results

The pulse energy ( $E$ ) and duration ( $\Delta t$ ) were measured for  $R = 40\%$  and a variety of pump powers, slab lengths and cavity round-trip times, which was varied by moving the HR mirror. The inverse relationship between pulse energy and pulse duration is demonstrated in Fig. 8(left) by plotting  $1/\Delta t$  versus  $E$  for a range of round trip times ( $t_r$ ) when using the longer slab. The solid lines are linear fits.

The accuracy of the model is further demonstrated in Fig. 8(right), in which  $E\Delta t/A$  is plotted as a function of cavity round trip. The  $E\Delta t$  product was obtained by varying the pump energy so that a range of pulse energy and pulse duration combinations were obtained and the results were

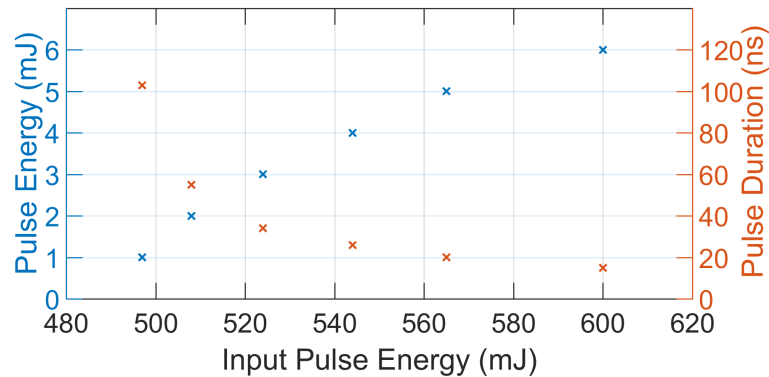


Fig. 7. Plot of the output energy and pulse duration versus input energy for the laser operated in Q-switched mode for the short 21 mm slab.

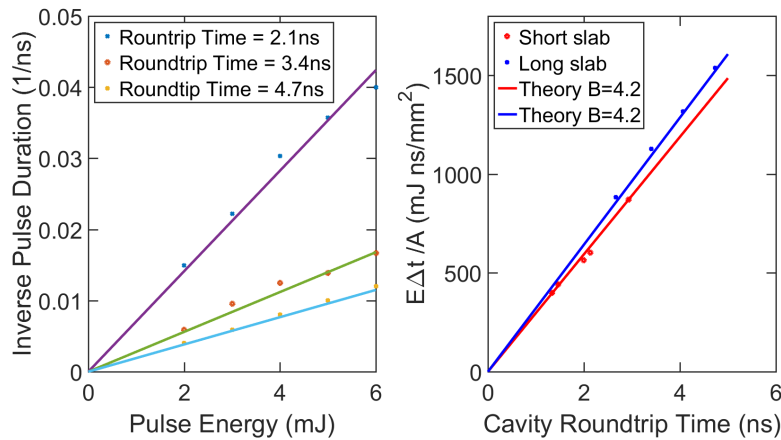


Fig. 8. Left: Plot of the inverse of pulse duration versus pulse energy for a range of different cavity round trip times. Right: Plot of the  $E\Delta t/A$  versus  $t_r$  for the two different slab lengths. The solid lines are predicted by Eq. (14) with the only free parameter being the beam overlap factor B

averaged. The error on the mean of these quantities was 5% or less. The mode area was obtained using a Gaussian resonator beam modeling package. Since the longer slab will lase at 1645 nm we used the parameters given in Table 1. For the shorter slab we use the parameters for 1617 nm which are  $\sigma = 2.9 \times 10^{-20} \text{ cm}^2$  and  $f_1 = 0.036$ . The only free parameter in the solid line in Fig. 8(right) was the beam overlap factor, B. To obtain an excellent fit we required the value of B to 4.2 rather than the expected value of 4. This difference can be explained by a 5% error in either the cross sections, area of the mode or the calibration of the power meter.

## 5. Conclusion

We have described a compact single-gain medium actively Q-switched Er:YAG laser that produced 14.5 ns, 6 mJ pulses. The laser used a CPFS gain medium end-pumped by a low spectral and spatial brightness 1470nm laser diode. Shorter pulses and the associated increase in their pulse energy were prevented by optical damage to the laser crystal.

We have also presented and experimentally validated a simple analytical theory that demonstrates that the product of pulse energy and duration of an actively Q-switched quasi-three-level lasers is constant when operated near threshold. This approximation is valid for most Er:YAG lasers because of the high pump intensity required to achieve threshold, and most quasi-three-level lasers that are operated at a high repetition rate.

Unfortunately, the model predicts that shorter duration pulses necessarily have higher fluence, which will result in laser induced damage. The only way to get shorter duration pulses is to further reduce the round trip time of the resonator.

### A. Derivation of Eq. (8)

The transcendental Eq. (6) can be combined with the definition of  $N_t$  (see Eq. (7)) to form the following equation:

$$0 = (N_i - N_f) - \frac{(f_2 + f_1)N_t - f_1 N_{eff}}{(f_1 + f_2)} \ln \left( \frac{f_2 N_i + f_1 N_t - f_1 N_{eff}}{f_2 N_f + f_1 N_t - f_1 N_{eff}} \right) \quad (16)$$

By introducing  $\Delta N_i = N_i - N_t$  and  $\Delta N_f = N_t - N_f$ , substituting them into Eq. (16) and then performing a second order Taylor's series expansion about  $\Delta N_f = \Delta N_i = 0$ , Eq. (16) can be re-written as:

$$0 = \frac{\Delta N_i^2 - \Delta N_f^2}{2(N_t(f_2 + f_1) - f_1 N_{eff})} = \frac{(N_i + N_f - 2N_t)(N_i - N_f)}{2(N_t(f_2 + f_1) - f_1 N_{eff})} \quad (17)$$

Eq. (17) is only valid above threshold ( $N_i > N_f$ ) if  $N_i + N_f - 2N_t = 0$ .

### Acknowledgments

The authors acknowledge Martin O'Connor and Gerry Smith from BAE Systems Australia (Holden Hill) for useful discussions. This work was financially supported by BAE Systems Australia and the Australian Research Council under ARC Linkage Grant LP110200734